

DR. CLÁUDIO NAHUM ALVES (Orcid ID : 0000-0001-6576-4229)

Article type : Research Article

Inhibition of Tyrosinase by 4H-Chromene Analogues: Synthesis, Kinetic Studies and Computational Analysis

Edikarlos M. Brasil^{1,7}, Luciana M. Canavieira¹, Érica T. C. Cardoso², Edilene O. Silva⁴, Jerônimo Lameira^{1,3}, José L. M. Nascimento^{2,3,*}, Vera L. Eifler-Lima⁵, Barbarella de Matos Macchi^{2,3}, Dharmarajan Sriram⁶, Paul V. Bernhardt⁷, José Rogério Araújo Silva¹, Craig M. Williams⁷ and Cláudio N. Alves^{1,3,*}

¹Laboratório de Planejamento e Desenvolvimento de Fármacos, Instituto de Ciências Exatas e Naturais, Universidade Federal do Pará, 66075-110, Belém, PA, Brazil. ²Laboratório de Neuroquímica Molecular e Celular, Instituto de Ciências Biológicas, Universidade Federal do Pará, 66075-110, Belém, PA, Brazil.

³Programa de Pós-Graduação em Biotecnologia, Universidade Federal do Pará, 66075-110, Belém, PA, Brazil.

⁴Laboratório de Biologia Estrutural, Instituto de Ciências Biológicas, Universidade Federal do Pará, 66075-110, Belém, PA, Brazil.

⁵Faculdade de Farmácia, Universidade Federal do Rio Grande do Sul, Avenida Ipiranga 2752, 90610-000 Porto Alegre, Rio Grande do Sul, Brazil.

This article has been accepted for publication and undergone full peer review but has not been through the copyediting, typesetting, pagination and proofreading process, which may lead to differences between this version and the Version of Record. Please cite this article as doi: 10.1111/cbdd.13001

This article is protected by copyright. All rights reserved.

⁶Medicinal Chemistry and Antimycobacterial Research Laboratory, Department of Pharmacy, Birla Institute of Technology and Science, Pilani, Hyderabad Campus, Jawahar Nagar, Hyderabad 500 078, India.

⁷School of Chemistry and Molecular Biosciences, University of Queensland, Brisbane, 4072, Queensland, Australia.

Keywords: Tyrosinase; Kojic Acid; Multicomponent Reaction; Inhibitor; Kinetic Assays; Molecular Modeling.

Corresponding author:

*Phone: (+55) 91-3201-8235. Fax: (+55) 91-3201-8235. E-mail: nahum@ufpa.br

*Phone: (+55) 91-3201-1601. Fax: (+55) 91-3201-7633. E-mail: jlmn@ufpa.br

Running Title: Developing new inhibitors with Tyrosinase activity via synthetic and computational techniques.

Abstract

Inhibition of mushroom tyrosinase was observed with synthetic dihydropyrano[3,2-*b*]chromenediones. Among them, DHPC04 displayed the most potent tyrosinase inhibitory activity with a K_i value of 4 μ M, comparable to the reference standard inhibitor kojic acid. A kinetic study suggested that these synthetic heterocyclic compounds behave as competitive inhibitors for the L-DOPA binding site of the enzyme. Furthermore, molecular modeling provided important insight into the mechanism of binding interactions with the tyrosinase copper active site.

Introduction

Melanin is the major cellular component observed in many species of animals, plants, fungi and bacteria (1). In humans it is responsible for skin color and protection against radiation (2). However, abnormal accumulation of melanin induces pigmentation disorders, among which, the most deadly form of skin cancer can form (i.e. melanoma) (3). Melanin develops in pigment cells called melanocytes due to the overproduction of melanin, the protective tanning pigment in the skin (4).

Melanin biosynthesis is conducted in melanocytes, found in the basal layer of the epidermis and controlled by a binuclear copper enzyme called tyrosinase (TYR) (EC 1.14.14.1) (5). TYR is ubiquitous and catalyzes the oxidation of both monophenols (cresolase or monophenolase activity) and *o*-diphenols (catecholase or diphenolase activity) into reactive *o*-quinones. In addition, it is a rate-limiting enzyme for controlling the production of melanin. The melanogenesis begins with the conversion of the amino acid L-tyrosine to L-3,4-dihydroxyphenylalanine (L-DOPA) catalyzed by tyrosinase (TYR) (6). Therefore, the regulation of the TYR activity is directly connected with melanin biosynthesis.

TYR is classified structurally as a type-3 copper protein in which each active-site copper ion is coordinated by three histidine residues (7) (Figure 1). In general, the TYR inhibition mechanism is frequently based on both specific TYR inhibitors and specific TYR inactivators (8). A large set of potent TYR inhibitors from natural and synthetic resources have been reported during the last few years (8-12). Kojic acid (KA) is a well-known TYR inhibitor and is widely used as a popular cosmetic skin-lightening ingredient. Its capacity to chelate copper ion at the active site of the enzyme may consistently explain its inhibitory effect (13). However, it only showed slight inhibitory activity against pigmentation within intact melanocytes or in clinical assays (14). Therefore, it remains necessary to find new TYR inhibitors with higher activity and without off target side effects.

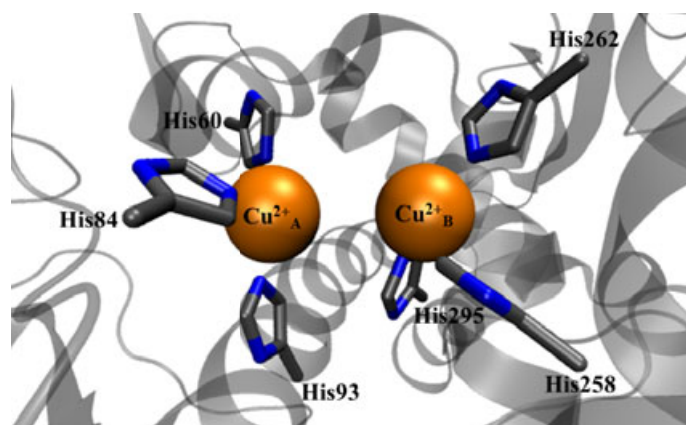


Figure 1. Catalytic site of TYR. The bivalent copper ions are chelated by three individual histidine residues.

Dihydropyrano[3,2-*b*]chromenediones (DHPCs), which are considered 4H-chromenes, are an important class of fused oxygenated heterocycles that are synthesised via a one-pot three-component reaction of kojic acid, an aldehyde and a 1,3-dione (15) (Figure 2). These heterocyclic compounds display a considerable structural diversity, including a strategic alcoholic hydroxyl functional group ($-\text{CH}_2\text{OH}$), which in turn can be modified by attaching biologically functional groups to develop more potent drug molecules. Interestingly, 4H-chromene derivatives present a wide range of biological properties, such as fungicidal (16), antitumor (17), antibacterial (18), antidepressant (19), antioxidative (20), and antihypertensive (21) activity.

In this study, we report the synthesis (including X-ray characterisation), inhibitory effect and computational modeling of dihydropyrano[3,2-*b*]chromenediones (DHPCs) as TYR inhibitors.

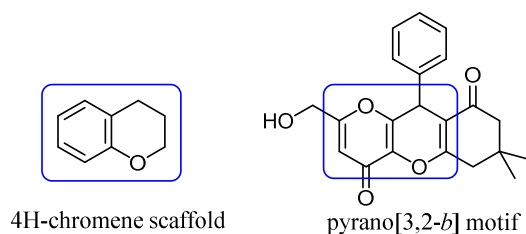


Figure 2. The 4H-chromene scaffold (left) and the pyrano[3,2-*b*] motif (right).

Materials and Methods

Experimental Section

Materials

TYR of mushroom (M.W. 128 kDa), L-DOPA, dimethylsulfoxide (DMSO) and KA were purchased from Sigma-Aldrich.

TYR Activity

TYR-inhibition activity of the DHPC01-04 compounds (Table 1) were performed by using L-DOPA as a substrate according to Kubo and co-workers (22) with slight modification. Incubation was carried out at 160 μ l of different concentrations of the substrate L-DOPA, 20 μ l (2.4 U) of enzyme mushroom tyrosinase, 20 μ l of KA and different concentrations of DHPCs (25, 50 and 100 μ M). All solutions were prepared in Phosphate Buffered Saline (PBS) pH 7.2.

The reaction was initiated by addition of enzyme to all wells simultaneously, which was measured over the first 5 minutes in the microplate reader (ELx800, BioTek) with a 490 nm filter. Furthermore, a control reaction was also performed by incubating the enzyme with KA or DHPCs in the absence of the substrate to demonstrate that there was no variation in absorbance over time.

Determination of Inhibition Constant (K_i)

The mode of inhibition on the enzyme was assayed by incubation of the different concentrations of L-DOPA (0; 0.25; 0.5; 0.75; 1.0; 2.0; 3.0 and 4.0 mM) and inhibitors (0; 0.001; 0.025; 0.05; 0.1; 0.2; 0.4; 0.8 and 1.6 mM). The kinetic parameters (K_m , V_{max} and K_i) were determined with the GraphPad Prism®5.0 software, according to the following equations:

I. Competitive Inhibition:

$$K_{m_{App}} = K_m \cdot \left(1 + \frac{I}{K_i}\right)$$

$$Y = \frac{V_{max} \cdot X}{K_m + X_{App}}$$

II. Mixed Inhibition:

$$V_{max_{App}} = \frac{V_{max}}{\left[1 + \frac{I}{(\alpha \cdot K_i)}\right]}$$

$$K_{m_{max_{App}}} = \frac{K_m \cdot \left(1 + \frac{I}{K_i}\right)}{\left[1 + \frac{I}{(\alpha \cdot K_i)}\right]}$$

$$Y = \frac{V_{max_{App}} \cdot X}{K_{m_{App}} + X}$$

where Y, X and I denotes average absorbance change *per* minute, concentration of L-DOPA and concentration of DHPCs, respectively. The parameter α determines mechanism, its value determines the degree to which the binding of inhibitor changes the affinity of the enzyme for substrate.

Computational Section

Molecular Docking

The crystal structure of tyrosinase from *A. bisporus* (*AbTYR*) was used as the initial point for computational procedures, it was obtained from the Protein Data Bank (PDB) under code 2Y9X (23), which contains tropolone (TRO) as a crystal inhibitor. In order to validate

the protocol and computational program used for molecular docking simulations for the proposed inhibitors, the crystal inhibitor (TRO) was re-docked in the active site of TYR. Then, the KA and DHPCs derivatives were submitted for docking calculations.

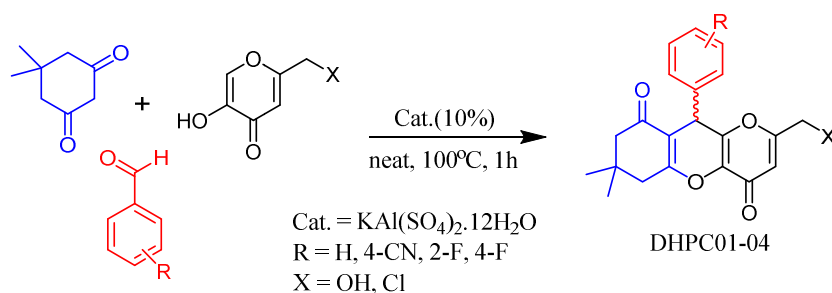
The molecular docking procedures were performed using the Molegro Virtual Docker (MVD) program (24). It has two docking search algorithms; MolDock Optimizer and MolDock SE (Simplex Evolution). The first is the default search algorithm in MVD (25), which is based on an evolutionary algorithm. However, MolDock SE performs better on some complexes where the standard MolDock algorithm fails (26). Accordingly, for previous computational analysis performed for TYR systems, the MolDock SE can be applied with success for this type of complex (27). The default parameters for the search algorithm were used to carry out molecular docking analysis. The detailed theory behind the MVD program and its characteristics are described elsewhere (24, 27).

Results and Discussion

4*H*-Chromene Analogues Synthesis

The synthesis of the dihydropyrano[3,2-*b*]chromenediones was successfully achieved by employing principles of “green chemistry”, and these included inexpensive off-the-shelf catalysts, short reaction times, solvent-free conditions, straightforward work-up, and good-to-high yielding syntheses (28).

For this study DHPCs were prepared in racemic form (mixture of enantiomers) via a three-component condensation reaction of an aromatic aldehyde, dimedone, and KA (28). To synthesize DHPC03 and DHPC04, chlorokojic acid (29) was used instead (Scheme 1). All compounds were fully characterized by ¹H NMR, ¹³C NMR, IR, HRMS and in some cases X-ray crystallography (see SI file).



Scheme 1. Synthesis of DHPC01 (R=H, X=OH), DHPC02 (R=4-CN, X=OH), DHPC03 (R=2-F, X=Cl), and DHPC04 (R=4-F, X=Cl).

Experimental Kinetic Assays and Inhibition

The kinetic analysis was determined from the equation of the Lineweaver-Burk to obtain the inhibition constant (K_i). The kinetic parameters showed that DHPC01 had a lower effect in TYR activity, and therefore, DHPC01 did not appear to inhibit mushroom TYR. Whereas, TYR activity was prominently inactivated by DHPC02, DHPC03 and DHPC04. The kinetic analysis showed that the value of V_{\max} remained the same and the value of K_m increased with increasing inhibitor concentrations, indicating that these molecules induced competitive inhibition (Figure 3). DHPC substrates might directly bind to the copper at the active site and thus compete with the L-DOPA substrate during catalysis.

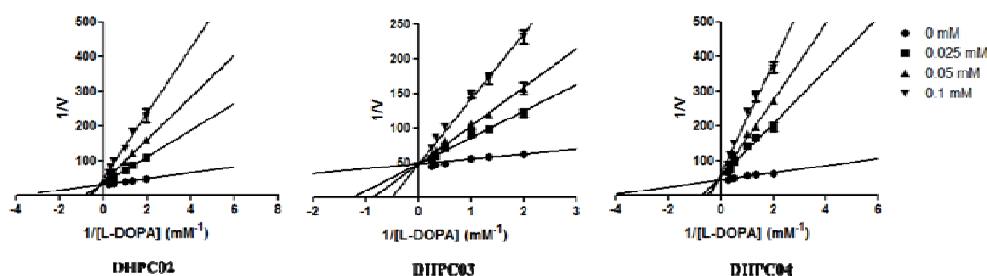


Figure 3. Plot of Lineweaver-Burk on the oxidation of L-DOPA by TYR and DHPC02, DHPC03 and DHPC04, respectively.

Accepted Article

Analysis of these kinetics parameters show that the K_i values of three compounds were 6.00 μM , 9.00 μM and 4.00 μM for DHPC02, DHPC03 and DHPC04, respectively (see Table 1). Therefore, these results show high rates of inhibition of TYR and the order appears to be DHPC04 > DHPC02 > DHPC03.

The increase in the slope of the graph $1/[S]$ indicated the binding strength of the competitive inhibitors. That is, the slope of the graph is increased by the factor $(1 + [I] / K_i)$ in the presence of the inhibitor. The kinetic analysis showed that these inhibitors have a single inhibition site, possibly with small differences in the docking site. Alternatively, these inhibitors can bind in multiple orientations within the catalytic site of the enzyme, giving an unexpected interactions, which may reflect small differences in inhibitor affinities.

The high slope value in the analysis of the variation in K_m as a function of inhibitor concentration: 22.12 ± 1.98 and $r^2 = 0.98$ for DHPC02; 19.92 ± 1.37 and $r^2 = 0.99$ for DHPC03; and 42.19 ± 7.58 and $r^2 = 0.94$ for DHPC04 (see Figure S4), suggests that these compounds have a single inhibition site of inhibition.

Finally, these findings quite reasonably suggest that the DHPC compounds bind to the same binding site as the substrate L-DOPA. The results match the values of affinity enzyme-inhibitor (K_i) and the values of free interaction energy. It is therefore likely that these inhibitors present kinetic parameters that show similar features derived from inhibitors with chelating and competitive properties (30).

Molecular Modelling Analysis

Molecular docking techniques have successfully been used to propose the bind mode and interactions occurring between the TYR enzyme and some potential inhibitors, such as, isophthalic acid (30), hesperetin (31), oxymatine (32), hydroxy-based thymol analogues (33), KA, and KA analogues (27). In this sense, we have performed similar analyses using the DHPC compounds derived from chemical synthesis. In order to validate the molecular docking procedure, and the MVD program, a re-docking calculation was computed using the crystal inhibitor (TRO) as a reference. Thus, comparing theoretical and experimental complexes (TYR-TRO) revealed excellent agreement between theoretical and experimental models. In this way, this molecular docking procedure was used to compute the favored conformation of the DHPC compounds in the binding site of the *Ab*TYR.

Accepted Article

According to the re-docking results, the TRO conformation obtained by molecular docking was in good agreement with its crystal structure conformation (see Figure S1). Furthermore, the DHPC compounds were also submitted to the same molecular docking steps. Our results showed that these compounds are complexed to the same binding pocket of the TRO inhibitor (see Figure S2), and that the MVD program can reproduce suitable conformations for molecular like KA and DHPC compounds in complex with the TYR enzyme.

During the synthesis of the DHPC compounds two enantiomers were obtained for each KA derivative (*R* and *S*). However, it is not clear at this stage which enantiomer is responsible for the TYR activity during kinetic analysis. In order to elucidate this aspect, molecular docking calculations using both enantiomers for all the DHPC compounds were undertaken. This information was taken into account with respect to the binding affinity values, and the interactions between the compounds and the amino acids residues of TYR.

The binding affinity values obtained through the MOLDOCK scoring function showed better affinity for the *R* enantiomer in all cases (Table 1). The binding affinity values for the *S* enantiomers are provided in the SI file. The orientation of the aryl group for this conformation allowed suitable interactions with part of TYR enzyme (Figure 4A). Since the aryl group for the *S* enantiomer was exposed to solvent the interaction with the residues of TYR disappeared (Figure 4B). Comparing KA with the DHPC compounds, all molecules interacted directly with one copper ion in the catalytic site of TYR as well as the TRO inhibitor (Figure 5), which supported the competitive inhibition proposal. Considering that DHPC04 had the strongest TYR inhibitory effect, our discussion at this point will be focused around this facet, although, it is representative of all other DHPC compounds.

Table 1. Experimental and theoretical binding affinity values.

Compound	K_i value*	MOLDOCK scoring (kcal·mol ⁻¹)
TRO	0.80 μ M**	-59.36
KA	5.00 μ M	-71.56
DHPC01	2.40 mM	-101.26
DHPC02	6.00 μ M	-107.82
DHPC03	9.00 μ M	-93.26
DHPC04	4.00 μ M	-102.32

*

Standard deviation for analyzed molecules are smaller than 0.01 (< 0.01) **Experimental value obtained by Espín and Wichers (34).

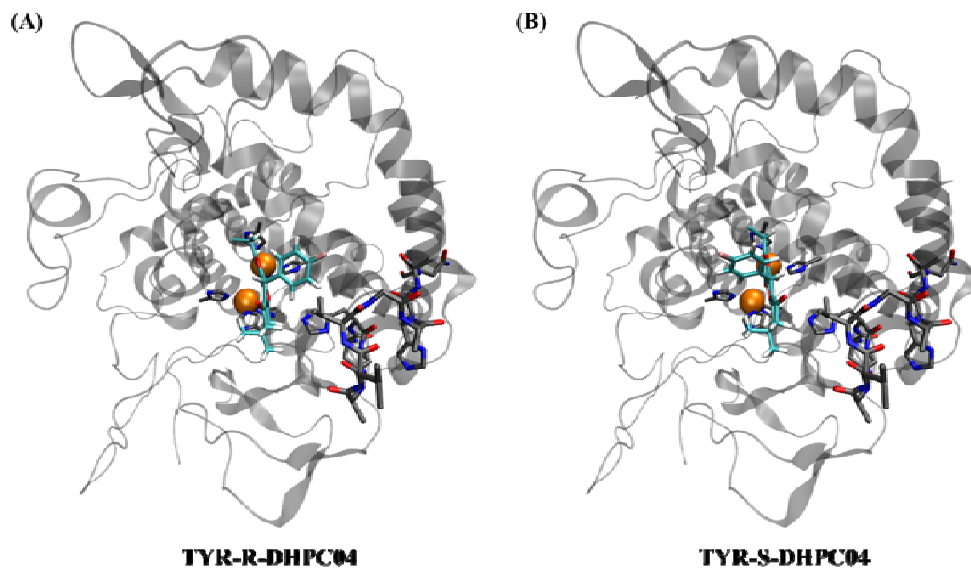


Figure 4. Binding mode of (A) R-DHPC04 and (B) S-DHPC04 con catalytic site of TYR. The loop which comprises residues Asn242-Asn252 are highlighted on the stick model. The binding mode of other DHPCs are present within the SI file (Figure S3).

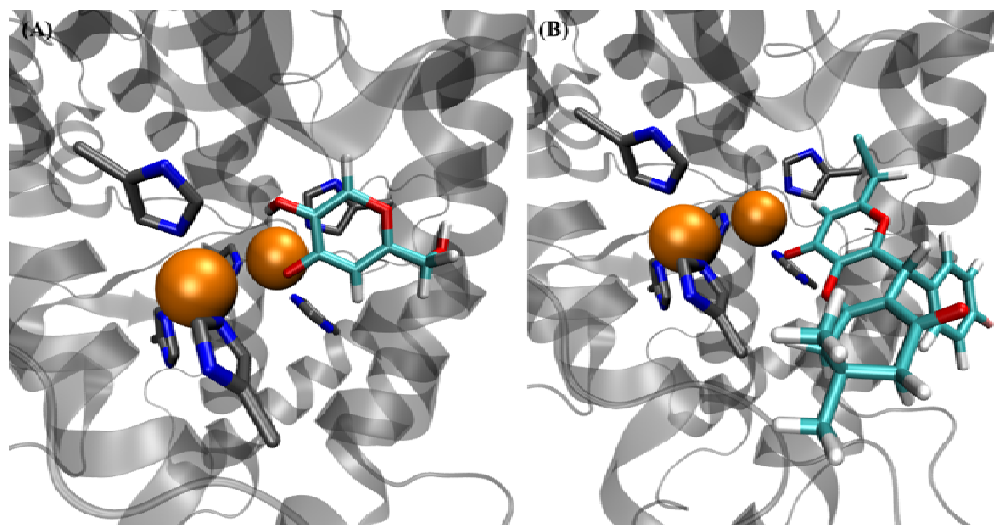


Figure 5. Binding mode of (A) KA and (B) R-DHPC04 catalytic site of TYR ranked by the MOLDOCK scoring function. The carbon atoms of inhibitors are in cyan color. Just the side chain of the His residues (stick model) and Cu^{2+} ions (ball model) are shown for clarity. The binding mode of other DHPCs are present within the SI file (Figure S2).

According to a previous computational analysis, the residues Met280 and Asn260 were found to be important in the first stage of inhibitor recognition, and their fixation during molecular docking and MD simulations (30, 35), respectively. Whether van der Waals interactions promoted by these residues are responsible is uncertain (30, 31, 36, 37). Our molecular docking results suggest that the same van der Waals interaction can be found, where the carbamoyl group of Asn260 interacts with nonpolar groups in the *para* position of KA and its derivatives for the *R* enantiomer.

Aside from the interactions promoted by the Asn260 residue, an interesting observation was the interaction between the DHPCs and the His243 residue, which could provide support for maintaining π - π interactions with the aryl ring of the DHPC compounds

(Figure 6). Interestingly, the DHPC compounds shown play a role in preventing the entry of the substrate into the active site. Once the aryl ring on the *R* enantiomer covers most of the TYR catalytic site, they maintain interactions with a loop of TYR which comprises the residues Asn242, His243, Gly244, Ala245, Val246, Val247, Gly248, Ala249, His250, Ala251 and Asn252 (Figure 4A). At this point, it is proposed that the DHPC compounds influence the molecular behavior of this part of the TYR enzyme, by preventing the entrance and recognition of the natural substrate.

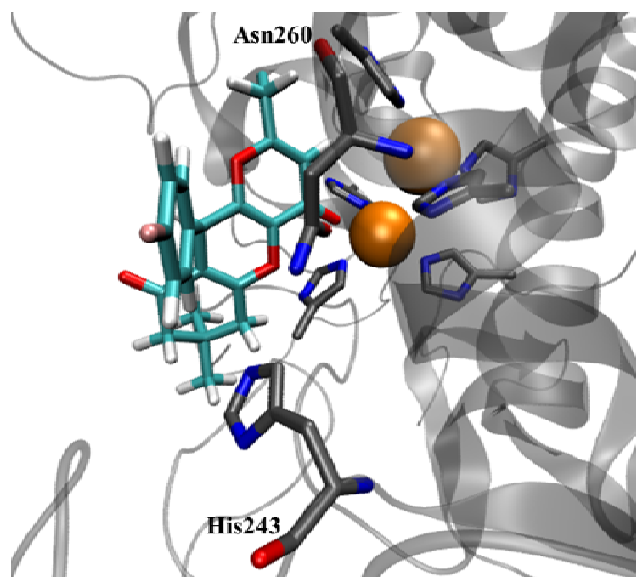


Figure 6. Interactions between the DHPC04 compound and residues His243 and Asn260 on the catalytic site of TYR. Carbon atoms of DHPC04 are in cyan color. The same interactions have been found for the other DHPC *R* enantiomers.

All DHPC compounds showed interactions with the copper ion in the catalytic site of TYR (Figure 5B). Moreover, van der Waals interactions were found between the aromatic groups of the DHPC compounds and residues Val247, Met256, Asn259, Phe263 and Val282 (Figure 7).

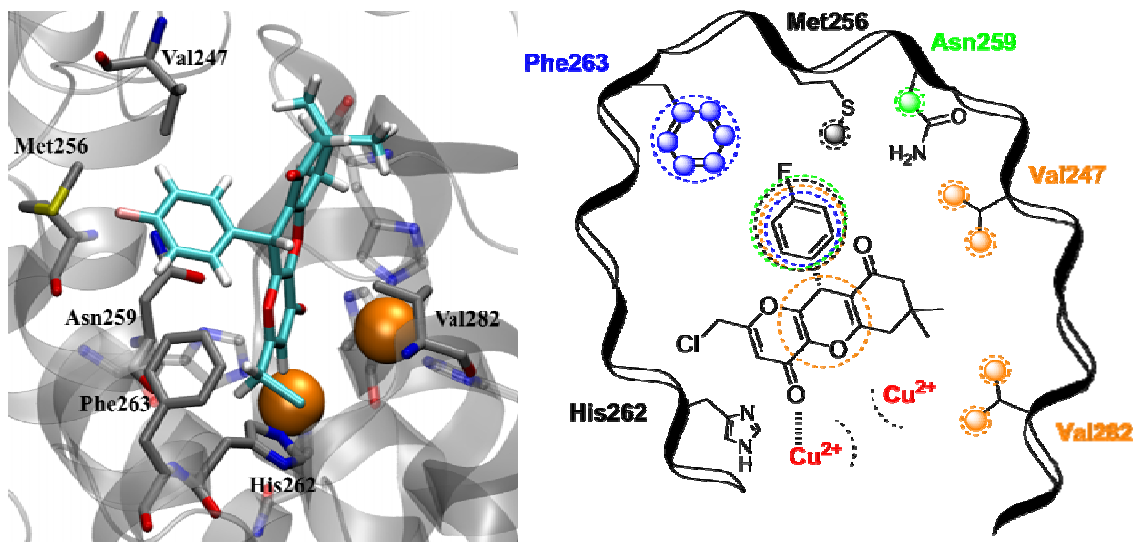


Figure 7. Van der Waals interactions between the DHPC04 compound and TYR residues. Carbon atoms of DHPC04 are in cyan color. The same interactions have been found for the others DHPC *R* enantiomers. In 2D scheme, colored dash circles represent van der Waals interactions; dashed line indicates copper ion chelated by carbonyl-oxygen atom.

Finally, Table 1 summarizes the affinity energy values computed by the MVD program for the TYR-inhibitor complexes. Despite, the MOLDOCK scoring function (26) not describing the relationship between the *in silico* and experimental data sufficiently well, it was found that the computed values are suitable for qualitative analysis in the case when multiple orientations are observed for the same compound. It is important to clarify that in the present work, the interest was only focused on predicting the position of the analogues within the active site of tyrosinase. Furthermore, for this application it was shown herein that the docking approach using the MVD program (24) provides suitable predictions for docked structures into the active site of tyrosinase. The computed energy values suggest that compounds DHPC02 and DHPC04 exhibit the highest affinity for the TYR catalytic site, with the same tendency as KA and the TRO inhibitors, which emphasise an inhibitory activity comprising a competitive mode [as well as their interaction with one of the catalytic copper ions (Cu^{2+} A)]. These results suggest that the binding site occupied by the DHPC compounds are very close to that found in previous studies (31, 35), therefore, the most probable inhibition action occurs via competition with the substrate L-DOPA in the TYR active site, which is in agreement with K_i values for competitive inhibition.

Conclusion

The inhibitory effect of various DHPC compounds were investigated against the TYR enzyme, which were found to induce changes in k_m . This is consistent with competitive inhibition interactions with the substrate (L-DOPA) at the active site. Correspondingly, changes in V_m indicated binding of the test compounds provided very effective to the inhibition of TYR in a competitive inhibitory manner. The inhibitory mechanism of such compounds is in accordance with the copper ion chelator concept, in that, analogues to kojic acid compete with L-DOPA in the active site,, which induces changes in the hydrophobic surfaces.

Therefore, a combination of inhibition kinetics and computational modeling may facilitate the testing of new potential TYR inhibitors and the prediction of their inhibitory mechanisms, as shown in the present study. Further biological evaluation of DHPCs and detailed toxicity studies are ongoing and will be reported in due course.

Supplementary Materials

Supplementary materials can be accessed at:
[http://onlinelibrary.wiley.com/journal/10.1111/\(ISSN\)1747-0285](http://onlinelibrary.wiley.com/journal/10.1111/(ISSN)1747-0285)

Acknowledgments

The authors gratefully acknowledge financial support from Conselho Nacional de Desenvolvimento Científico e Tecnológico (CNPq) and Coordenação de Aperfeiçoamento de Pessoal de Nível Superior (CAPES) for financial support. As well as the Center for High Performance Computing (CHPC) in Cape Town—South Africa—for computational support. Financial support by the University of Queensland, and the Australian Research Council (ARC) is gratefully acknowledged [C.M.W. (FT110100851)].

Conflicts of Interest

The authors declare no conflict of interest.

References

1. Slominski A, Tobin DJ, Shibahara S, Wortsman J (2004) Melanin pigmentation in mammalian skin and its hormonal regulation. *Physiological reviews*; **84**: 1155-228.
2. Seo SY, Sharma VK, Sharma N (2003) Mushroom tyrosinase: recent prospects. *Journal of agricultural and food chemistry*; **51**: 2837-53.
3. Saranga-Perry V, Ambe C, Zager JS, Kudchadkar RR (2014) Recent developments in the medical and surgical treatment of melanoma. *CA: a cancer journal for clinicians*; **64**: 171-85.
4. Rigel DS, Russak J, Friedman R (2010) The evolution of melanoma diagnosis: 25 years beyond the ABCDs. *CA: a cancer journal for clinicians*; **60**: 301-16.
5. Parveen I, Threadgill MD, Moorby JM, Winters A (2010) Oxidative phenols in forage crops containing polyphenol oxidase enzymes. *Journal of agricultural and food chemistry*; **58**: 1371-82.
6. Parvez S, Kang M, Chung HS, Bae H (2007) Naturally occurring tyrosinase inhibitors: mechanism and applications in skin health, cosmetics and agriculture industries. *Phytotherapy research : PTR*; **21**: 805-16.
7. Khan Mahmud Tareq H. (2007) Molecular design of tyrosinase inhibitors: A critical review of promising novel inhibitors from synthetic origins. *Molecular design of tyrosinase inhibitors: A critical review of promising novel inhibitors from synthetic origins*. p. 2277.
8. Chang TS (2009) An updated review of tyrosinase inhibitors. *International journal of molecular sciences*; **10**: 2440-75.
9. Kim YJ, Uyama H (2005) Tyrosinase inhibitors from natural and synthetic sources: structure, inhibition mechanism and perspective for the future. *Cellular and molecular life sciences : CMLS*; **62**: 1707-23.
10. Solano F, Briganti S, Picardo M, Ghanem G (2006) Hypopigmenting agents: an updated review on biological, chemical and clinical aspects. *Pigment cell research / sponsored by the European Society for Pigment Cell Research and the International Pigment Cell Society*; **19**: 550-71.
11. Bao K, Dai Y, Zhu ZB, Tu FJ, Zhang WG, Yao XS (2010) Design and synthesis of biphenyl derivatives as mushroom tyrosinase inhibitors. *Bioorganic & medicinal chemistry*; **18**: 6708-14.
12. Khan MT (2012) Novel tyrosinase inhibitors from natural resources - their computational studies. *Current medicinal chemistry*; **19**: 2262-72.
13. Cabanes J, Chazarra S, Garcia-Carmona F (1994) Kojic acid, a cosmetic skin whitening agent, is a slow-binding inhibitor of catecholase activity of tyrosinase. *The Journal of pharmacy and pharmacology*; **46**: 982-5.
14. Jimbow K, Obata H, Pathak MA, Fitzpatrick TB (1974) Mechanism of depigmentation by hydroquinone. *The Journal of investigative dermatology*; **62**: 436-49.
15. Reddy BVS, Reddy MR, Narasimhulu G, Yadav JS (2010) InCl₃-catalyzed three-component reaction: a novel synthesis of dihydropyrano[3,2-b]chromenediones under solvent-free conditions. *Tetrahedron Letters*; **51**: 5677-9.
16. Meepagala KM, Schrader KK, Burandt CL, Wedge DE, Duke SO (2010) New class of algicidal compounds and fungicidal activities derived from a chromene amide of Amyris texana. *Journal of agricultural and food chemistry*; **58**: 9476-82.
17. Raj T, Bhatia RK, Kapur A, Sharma M, Saxena AK, Ishar MP (2010) Cytotoxic activity of 3-(5-phenyl-3H-[1,2,4]dithiazol-3-yl)chromen-4-ones and 4-oxo-4H-chromene-3-carbothioic acid N-phenylamides. *European journal of medicinal chemistry*; **45**: 790-4.

18. Kumar D, Reddy VB, Sharad S, Dube U, Kapur S (2009) A facile one-pot green synthesis and antibacterial activity of 2-amino-4H-pyrans and 2-amino-5-oxo-5,6,7,8-tetrahydro-4H-chromenes. *European journal of medicinal chemistry*; **44**: 3805-9.
19. Le Bourdonnec B, Windh RT, Ajello CW, Leister LK, Gu M, Chu GH, et al. (2008) Potent, orally bioavailable delta opioid receptor agonists for the treatment of pain: discovery of N,N-diethyl-4-(5-hydroxyspiro[chromene-2,4'-piperidine]-4-yl)benzamide (ADL5859). *Journal of medicinal chemistry*; **51**: 5893-6.
20. Machado NFL, Marques MPM (2010) Bioactive Chromone Derivatives – Structural Diversity. *Current Bioactive Compounds*; **6**: 76-89.
21. Johannes CW, Visser MS, Weatherhead GS, Hoveyda AH (1998) Zr-Catalyzed Kinetic Resolution of Allylic Ethers and Mo-Catalyzed Chromene Formation in Synthesis. Enantioselective Total Synthesis of the Antihypertensive Agent (S,R,R,R)-Nebivolol. *Journal of the American Chemical Society*; **120**: 8340-7.
22. Kubo I, Kinst-Hori I, Chaudhuri SK, Kubo Y, Sanchez Y, Ogura T (2000) Flavonols from *Heterotheca inuloides*: tyrosinase inhibitory activity and structural criteria. *Bioorganic & medicinal chemistry*; **8**: 1749-55.
23. Ismaya WT, Rozeboom HJ, Weijn A, Mes JJ, Fusetti F, Wichers HJ, et al. (2011) Crystal structure of *Agaricus bisporus* mushroom tyrosinase: identity of the tetramer subunits and interaction with tropolone. *Biochemistry*; **50**: 5477-86.
24. Thomsen R, Christensen MH (2006) MolDock: a new technique for high-accuracy molecular docking. *Journal of medicinal chemistry*; **49**: 3315-21.
25. Gehlhaar DK, Bouzida D, Rejto PA. (1998) Fully automated and rapid flexible docking of inhibitors covalently bound to serine proteases. In: Porto VW, Saravanan N, Waagen D, Eiben AE, editors *Fully automated and rapid flexible docking of inhibitors covalently bound to serine proteases*. Berlin, Heidelberg: Springer Berlin Heidelberg: p. 449-61.
26. Zaheer ul H, Khan W (2011) Molecular and structural determinants of adamantyl susceptibility to HLA-DRs allelic variants: an in silico approach to understand the mechanism of MLEs. *Journal of computer-aided molecular design*; **25**: 81-101.
27. Lima CR, Silva JR, de Tassia Carvalho Cardoso E, Silva EO, Lameira J, do Nascimento JL, et al. (2014) Combined kinetic studies and computational analysis on kojic acid analogous as tyrosinase inhibitors. *Molecules*; **19**: 9591-605.
28. Li WL, Wu LQ, Yan FL (2011) Alum-catalyzed one-pot synthesis of dihydropyrano[3,2-b]chromenediones. *Journal of the Brazilian Chemical Society*; **22**: 2202-5.
29. Ma Y, Luo W, Quinn PJ, Liu Z, Hider RC (2004) Design, synthesis, physicochemical properties, and evaluation of novel iron chelators with fluorescent sensors. *Journal of medicinal chemistry*; **47**: 6349-62.
30. Si YX, Yin SJ, Park D, Chung HY, Yan L, Lu ZR, et al. (2011) Tyrosinase inhibition by isophthalic acid: kinetics and computational simulation. *International journal of biological macromolecules*; **48**: 700-4.
31. Si YX, Wang ZJ, Park D, Chung HY, Wang SF, Yan L, et al. (2012) Effect of hesperetin on tyrosinase: inhibition kinetics integrated computational simulation study. *International journal of biological macromolecules*; **50**: 257-62.
32. Liu XX, Sun SQ, Wang YJ, Xu W, Wang YF, Park D, et al. (2013) Kinetics and computational docking studies on the inhibition of tyrosinase induced by oxymatrine. *Applied biochemistry and biotechnology*; **169**: 145-58.
33. Ashraf Z, Rafiq M, Seo SY, Kwon KS, Babar MM, Zaidi NU (2015) Kinetic and in silico studies of novel hydroxy-based thymol analogues as inhibitors of mushroom tyrosinase. *European journal of medicinal chemistry*; **98**: 203-11.

- Accepted Article
34. Espin JC, Wichers HJ (1999) Slow-binding inhibition of mushroom (*Agaricus bisporus*) tyrosinase isoforms by tropolone. *Journal of agricultural and food chemistry*; **47**: 2638-44.
 35. Hu WJ, Yan L, Park D, Jeong HO, Chung HY, Yang JM, et al. (2012) Kinetic, structural and molecular docking studies on the inhibition of tyrosinase induced by arabinose. *International journal of biological macromolecules*; **50**: 694-700.
 36. Yin SJ, Si YX, Qian GY (2011) Inhibitory effect of phthalic Acid on tyrosinase: the mixed-type inhibition and docking simulations. *Enzyme research*; **2011**: 294724.
 37. Munoz-Munoz JL, Garcia-Molina F, Varon R, Garcia-Ruiz PA, Tudela J, Garcia-Canovas F, et al. (2010) Suicide inactivation of the diphenolase and monophenolase activities of tyrosinase. *IUBMB life*; **62**: 539-47.